

Chemometrics modeling, inverse docking and molecular simulations-driven design and multi-layered prioritization lead identification of novel analogs based on 2-aminobenzimidazole scaffolds for addressing Leishmaniasis

Presented

by

Arpita Biswas

PhD Research Scholar

Dept of Pharm Tech

Jadavpur University, Kolkata-700032

DDD LAB

Drug Discovery and Development
Laboratory

Under the guidance of

Dr. Probir Kumar Ojha

Associate Professor

Dept. Of Pharm. Tech

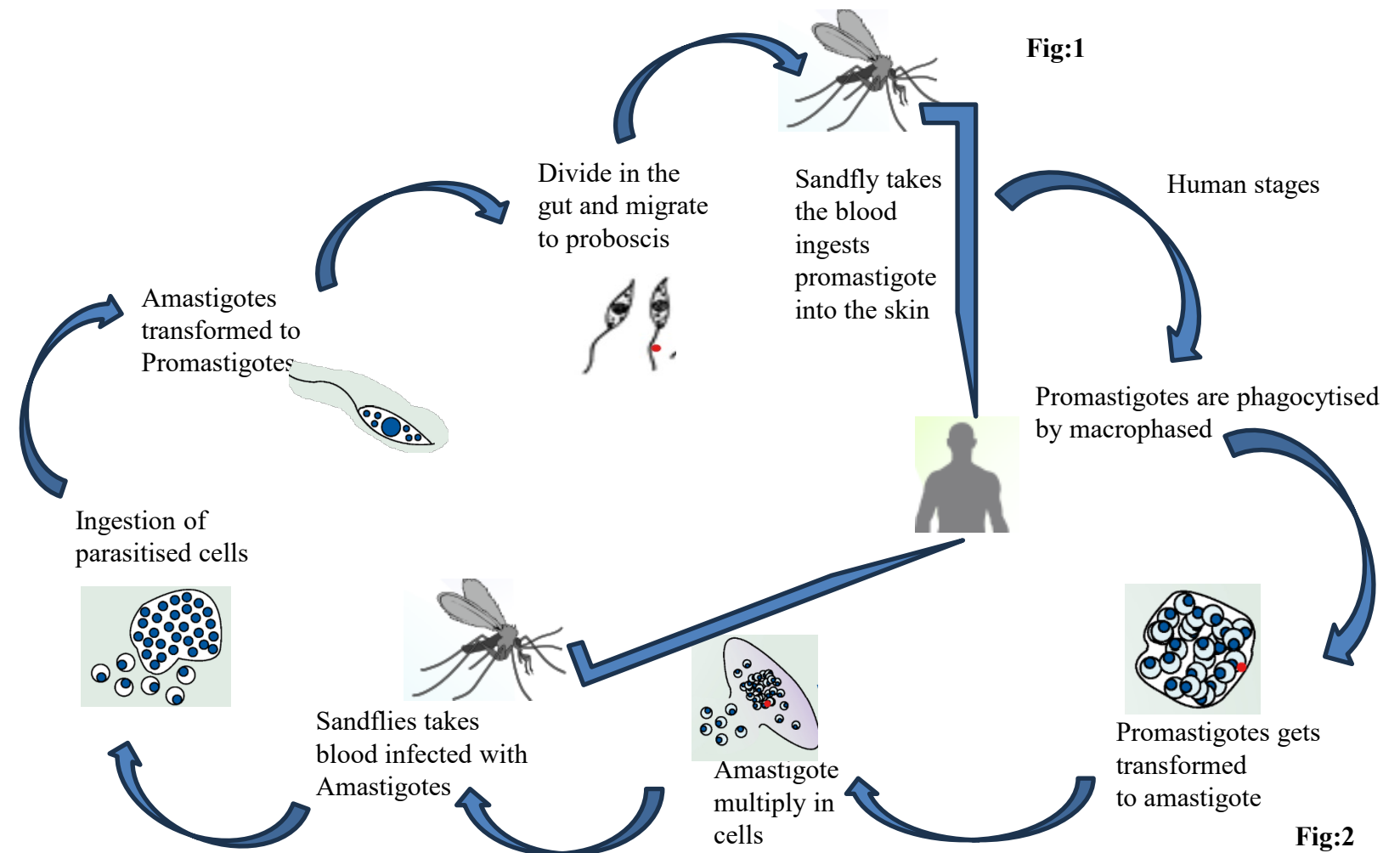
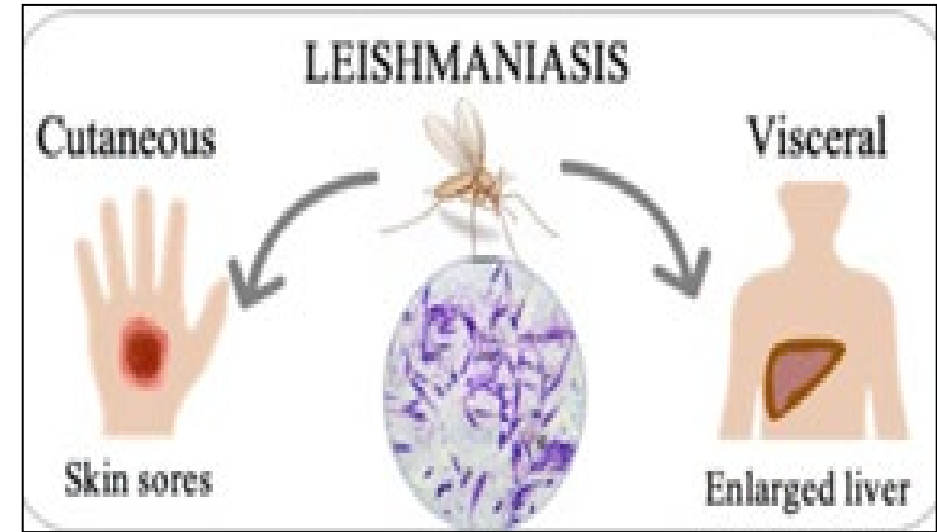
Jadavpur University, Kolkata-700032



It's a Threat to the mankind

Theme of 2023 NTD is-”Act Now. Act Together. Invest in Neglected Tropical Disease”

- Kala-azar (visceral leishmaniasis)-fatal if untreated, **Fig: 1**.
- **Causes:** Protozoan parasites which are transmitted by the bite of infected female phlebotomine sand-flies.
- Very limited no. of drugs available in the market.
- Having good extent of toxicity.
- Huge population gets affected.



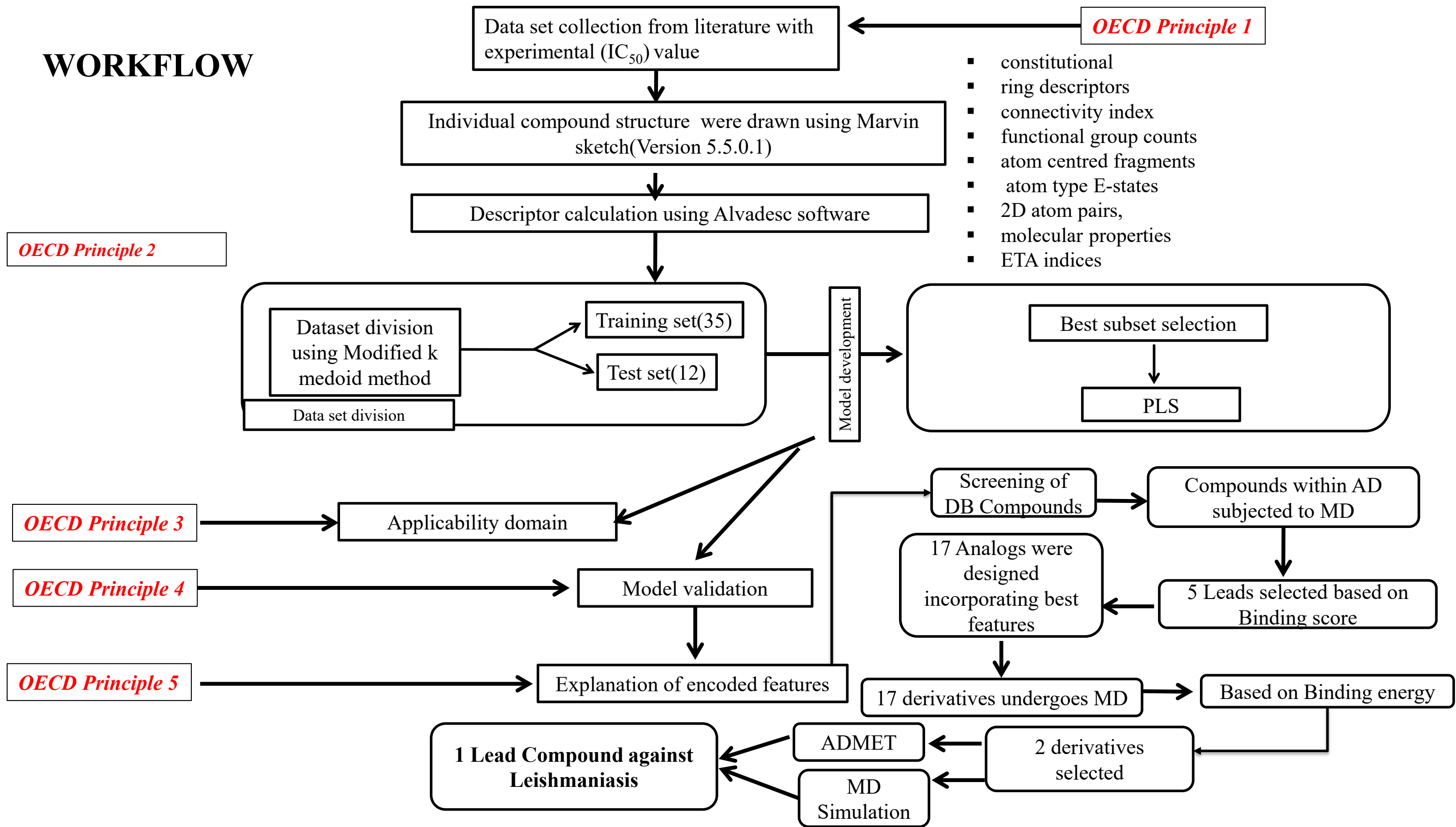
Flowchart of the lifecycle of parasite.(Amastigotes and Promastigotes), **Fig: 2**

Fig:2

Objective

- Design of new compounds with 2-aminobenzimidazole scaffold to counteract NTD endemic diseases.
- Development of QSAR-regression based predictive models which correlates biological activity with chemicals of molecular structure represented as descriptors is aimed to develop through various statistical approaches.
- Validation of developed models using globally accepted internal and external validation parameters.
- Screening of drugbank compounds using the validated model to develop new chemical compound with least toxicity against leishmaniasis

WORKFLOW



Results and discussion

PLS Model

Statistical parameters of the model is mentioned in the tabular form as Table:1

$$\text{pIC}_{50} = 1.41855 + 2.53073 * \text{Eta_F_A} - 0.61002 * \text{B10[C - N]} + 0.08752 * \text{F03[C - N]} + 0.29798 * \text{F06[N - F]}$$

Table:1

Model	LV	Training set(n=35)				Test set(n=12)					
		R^2	$Q^2_{(LOO)}$	$r_m^2_{(LOO)}$	$MAE_{(LOO)}$	Q^2_{F1}	Q^2_{F2}	$r_m^2_{(test)}$	$\Delta r_m^2_{(test)}$	CCC	MAE
PLS	2	0.688	0.611	0.497	0.240	0.735	0.698	0.525	0.235	0.800	0.211

Descriptors Contribution

4 Descriptors are found to have contribution towards developed model:

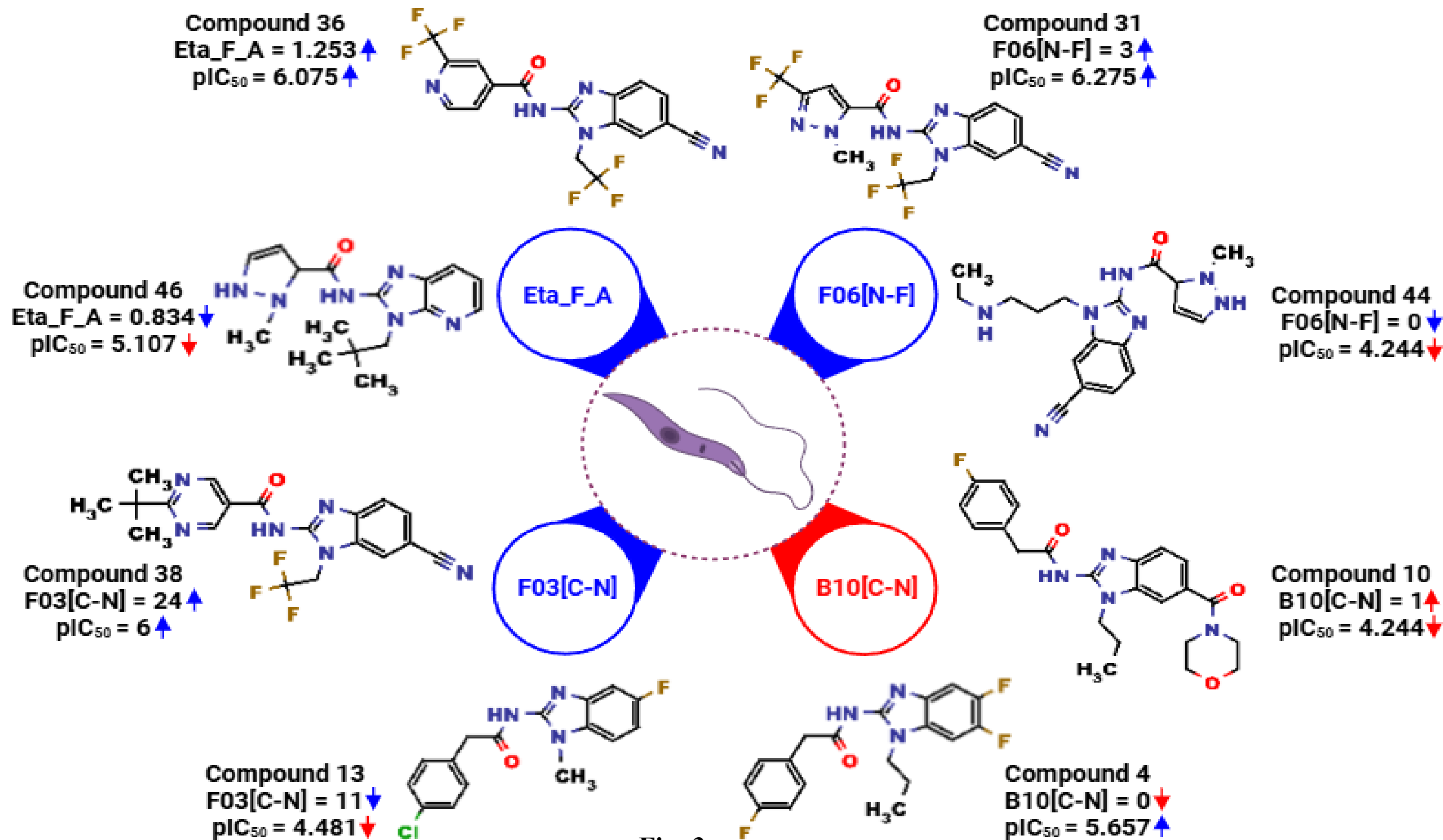


Fig: 3

PLS PLOT

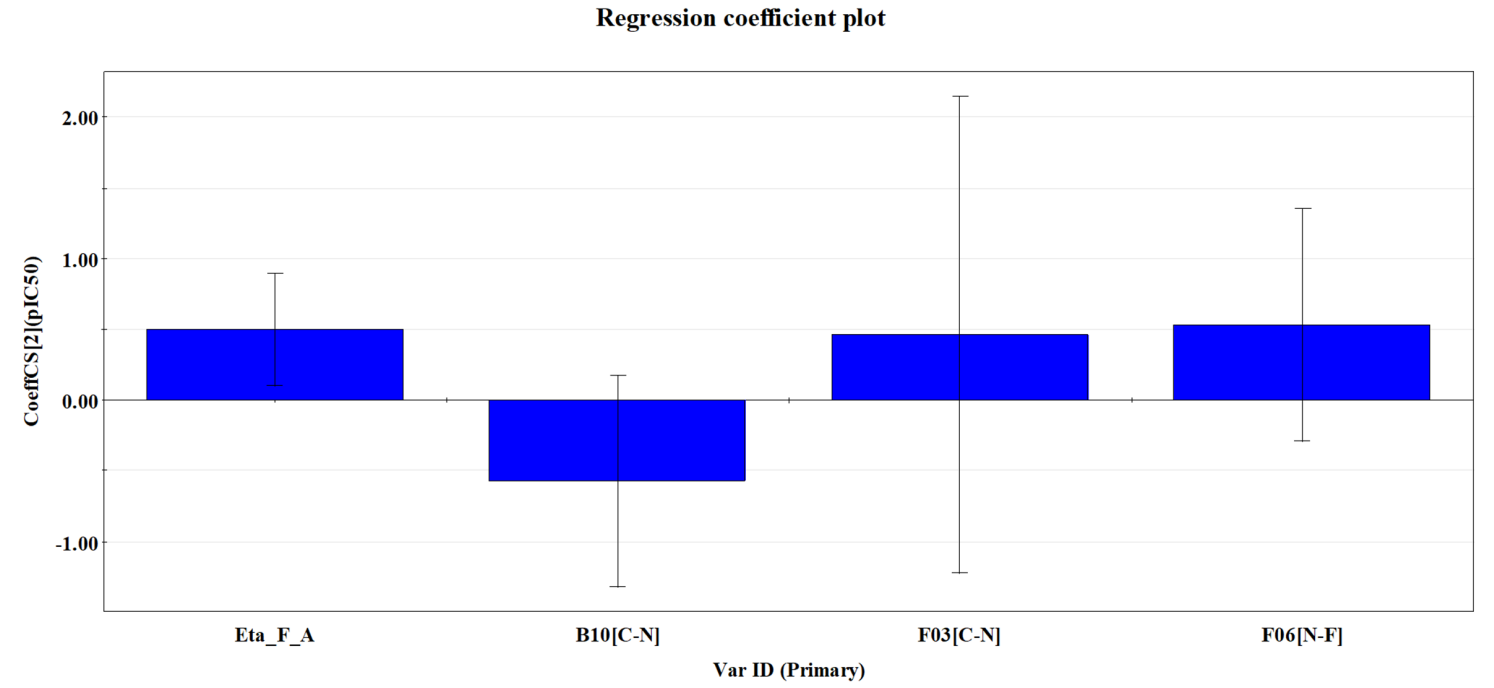
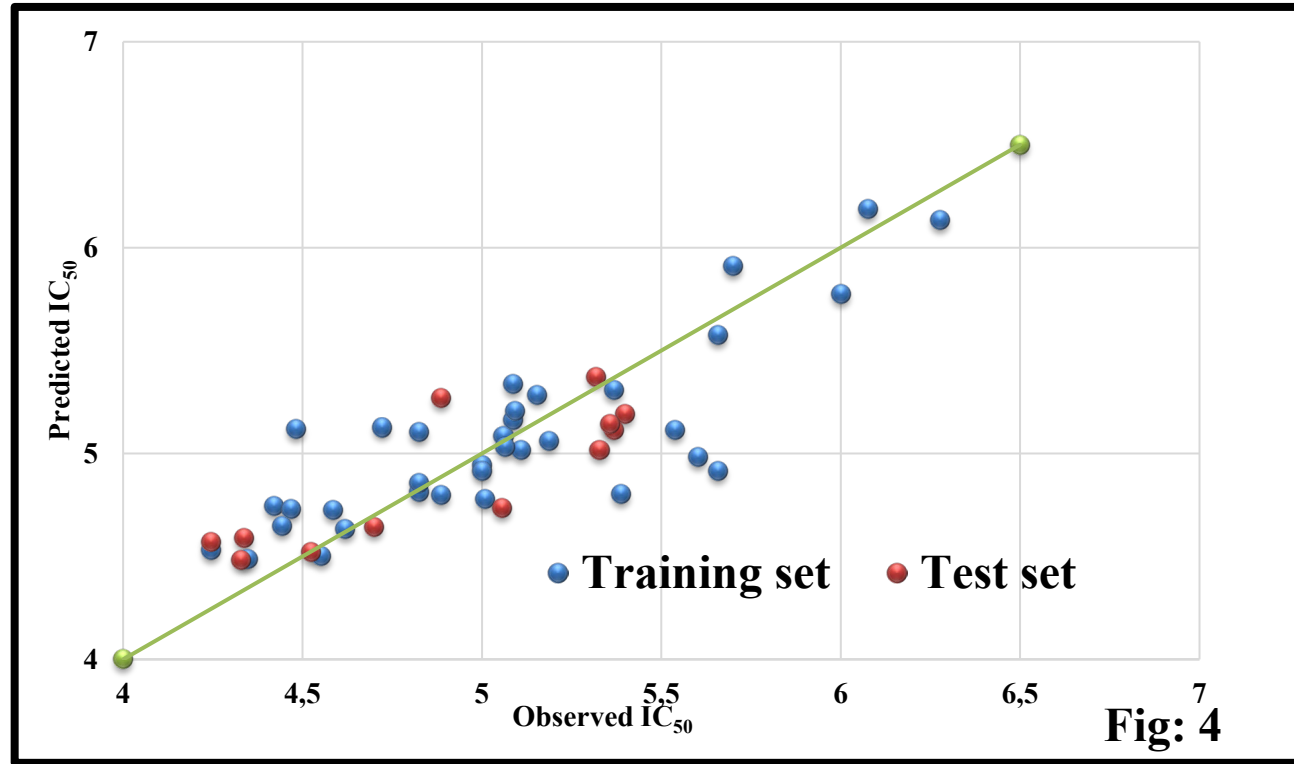


Fig: 5

VIP plot

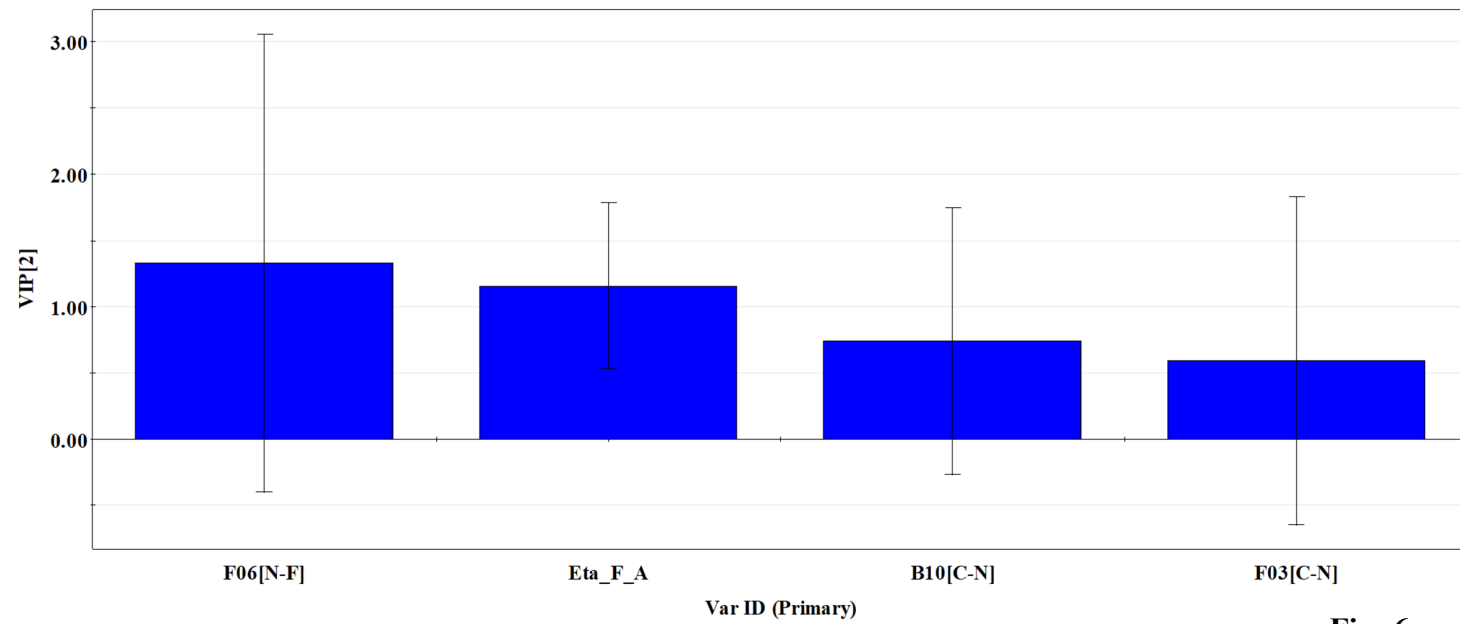


Fig: 6

Score plot

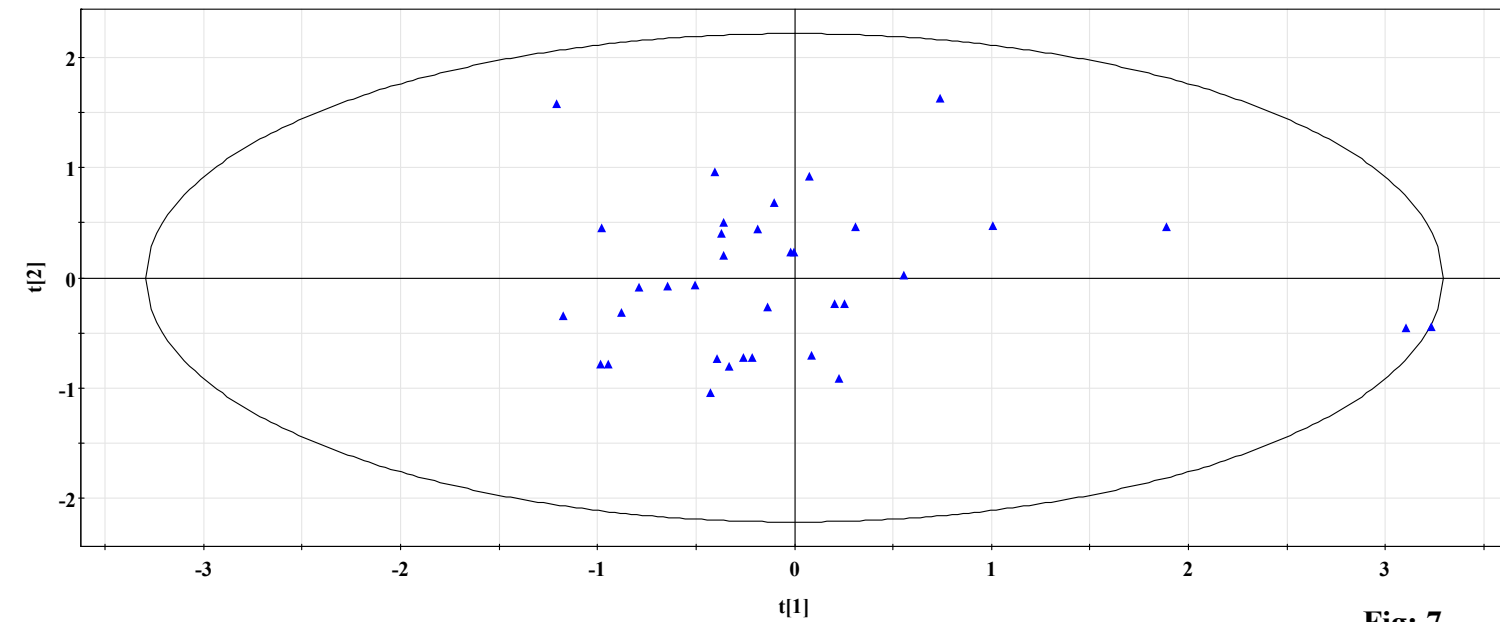


Fig: 7

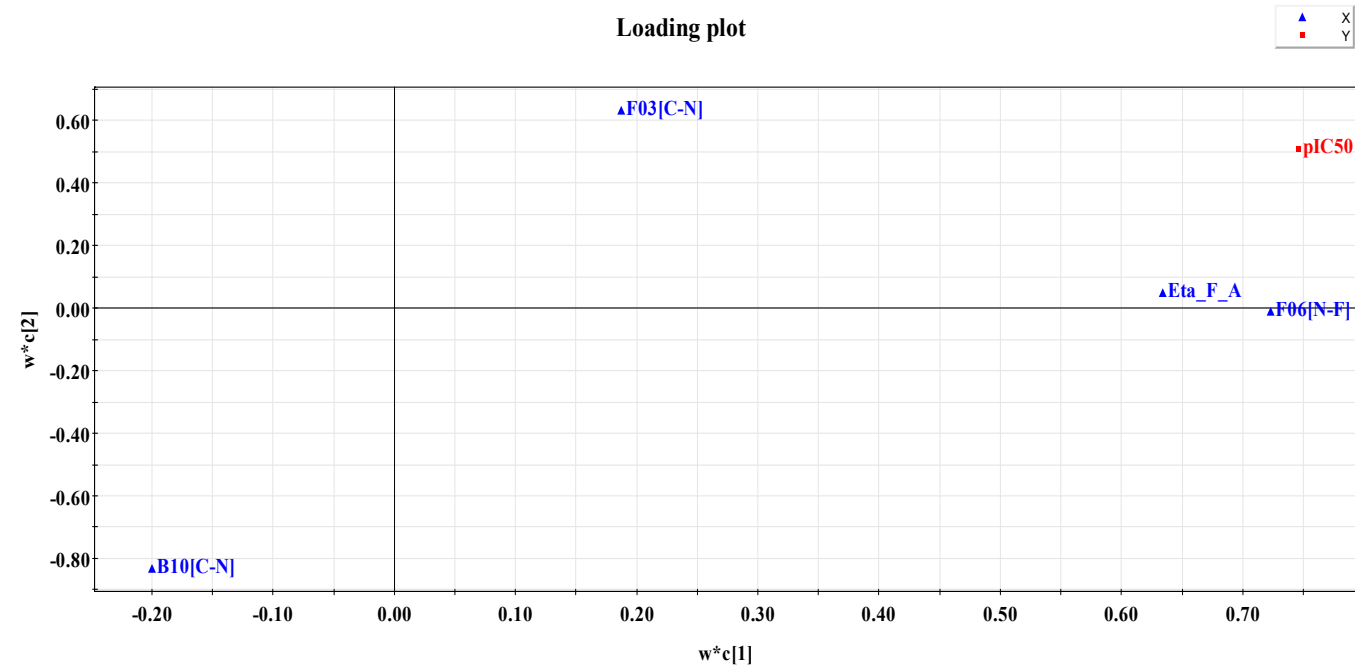
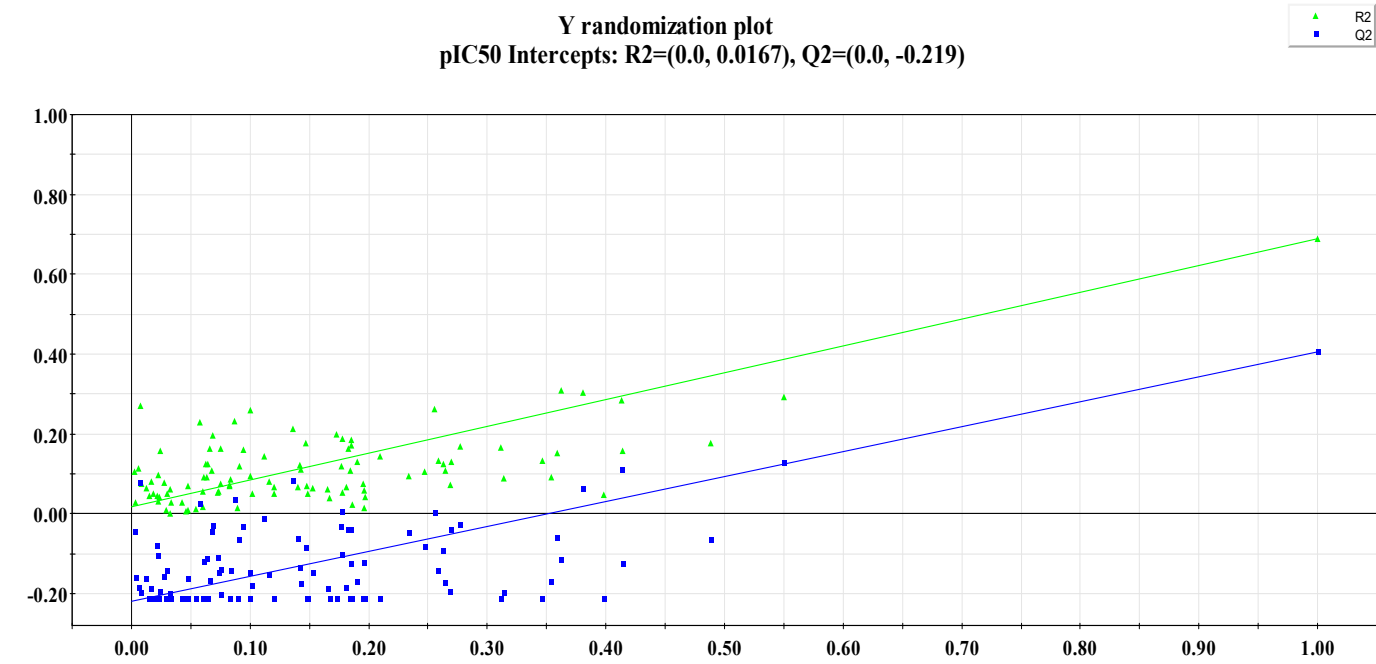


Fig: 8



100 permutations 2 components

Fig: 9

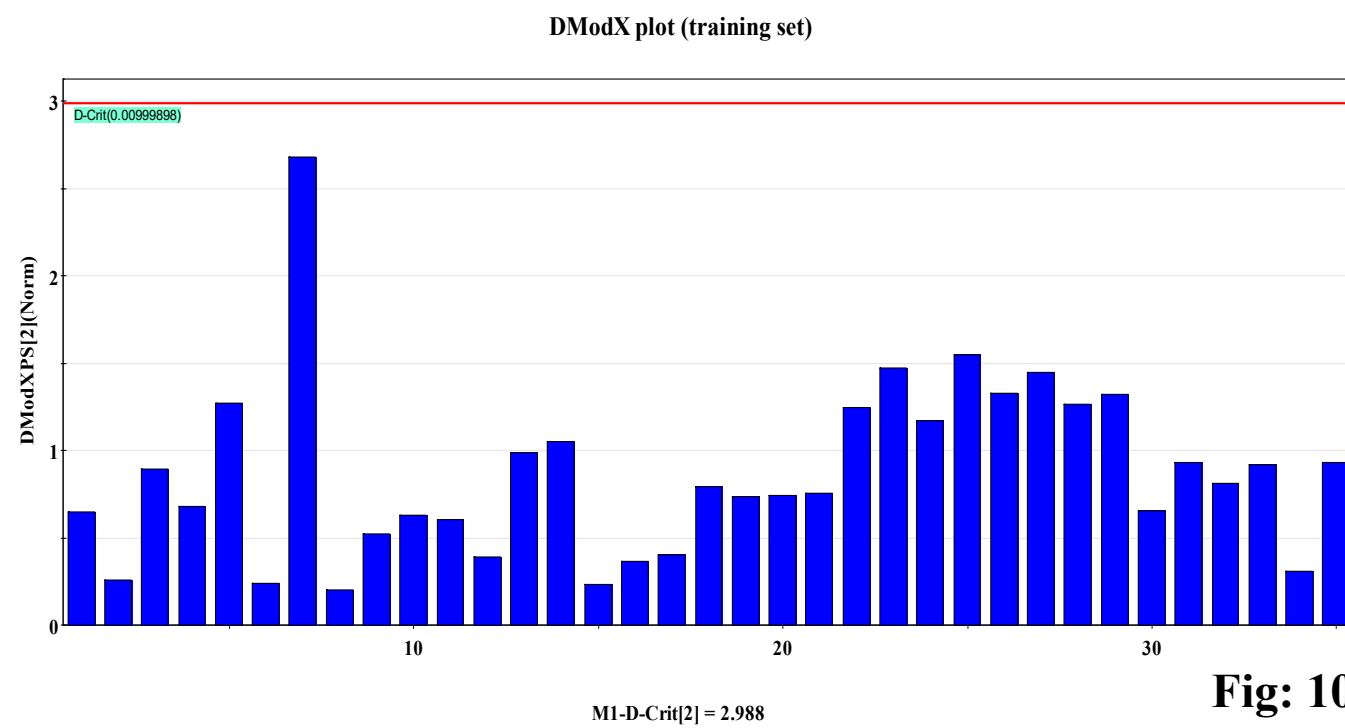


Fig: 10

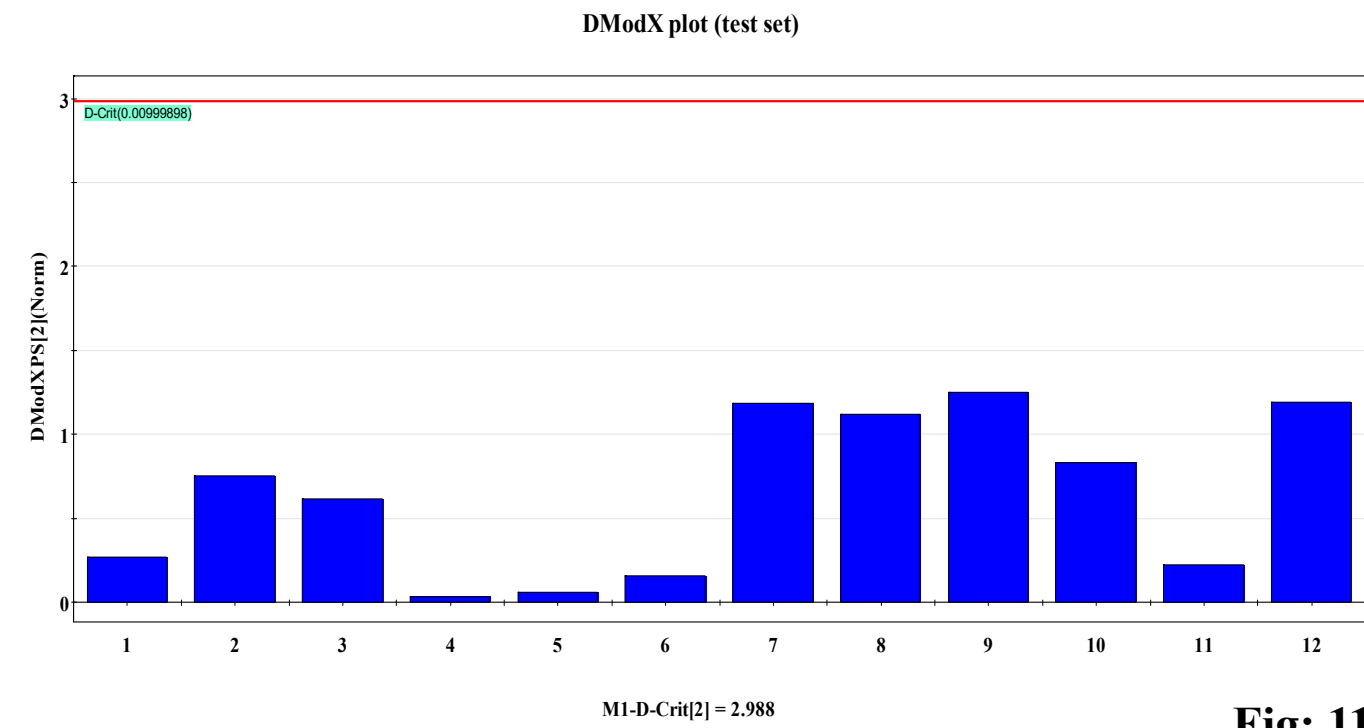


Fig: 11

Step-wise generation of Lead Analog against leishmaniasis

- The PLS Model generated was used to screen the DrugBank compounds based on AD.
- The compounds obtained again screened using R05 violation.
- The screened compounds now subjected to molecular docking using 15 targeted proteins.
- The docking results shows that the best binding score was obtained against TR.
- The screened compounds were assessed for their localization within the binding site of 15 putative protein targets to prioritize leads compounds based on their binding affinity.
- Inverse Docking, a tabular form of presented with target proteins against leishmaniasis, represented as,

Table:2

Target Proteins	Highest Binding score
TR	-6.58
AdoMetDC	-6.45
ARG	-5.95
FPS	-6.37
GspS	-6.40
NDkb	-6.49
ODC	-6.40
OPB	-6.42
S14D	-6.31
S24CM	-6.09
SpdS	-6.45
SS	-6.47
TS	-6.45
TXN	-6.47
TXNPx	-5.12

- 124 Compounds were found with highest dock score exceeding experimental TR inhibitor with TRL190
- Considering binding energy, top 5 leads against TR was identified, as mentioned on the table below., Table:3
- Positively correlated features escalating TR inhibitory activity obtained from QSAR study incorporated rationally to the generation of analogs.
- Thus resulting in 17 Analogs generation.

Table: 3

DrugBank ID	Binding energy
DB12269	-6.58185
DB01705	-6.38635
DB12457	-6.32147
DB03231	-6.0676
DB04260	-6.01953
MWW	-4.70903

Structures of 17 Analogs with 5 Lead Compounds

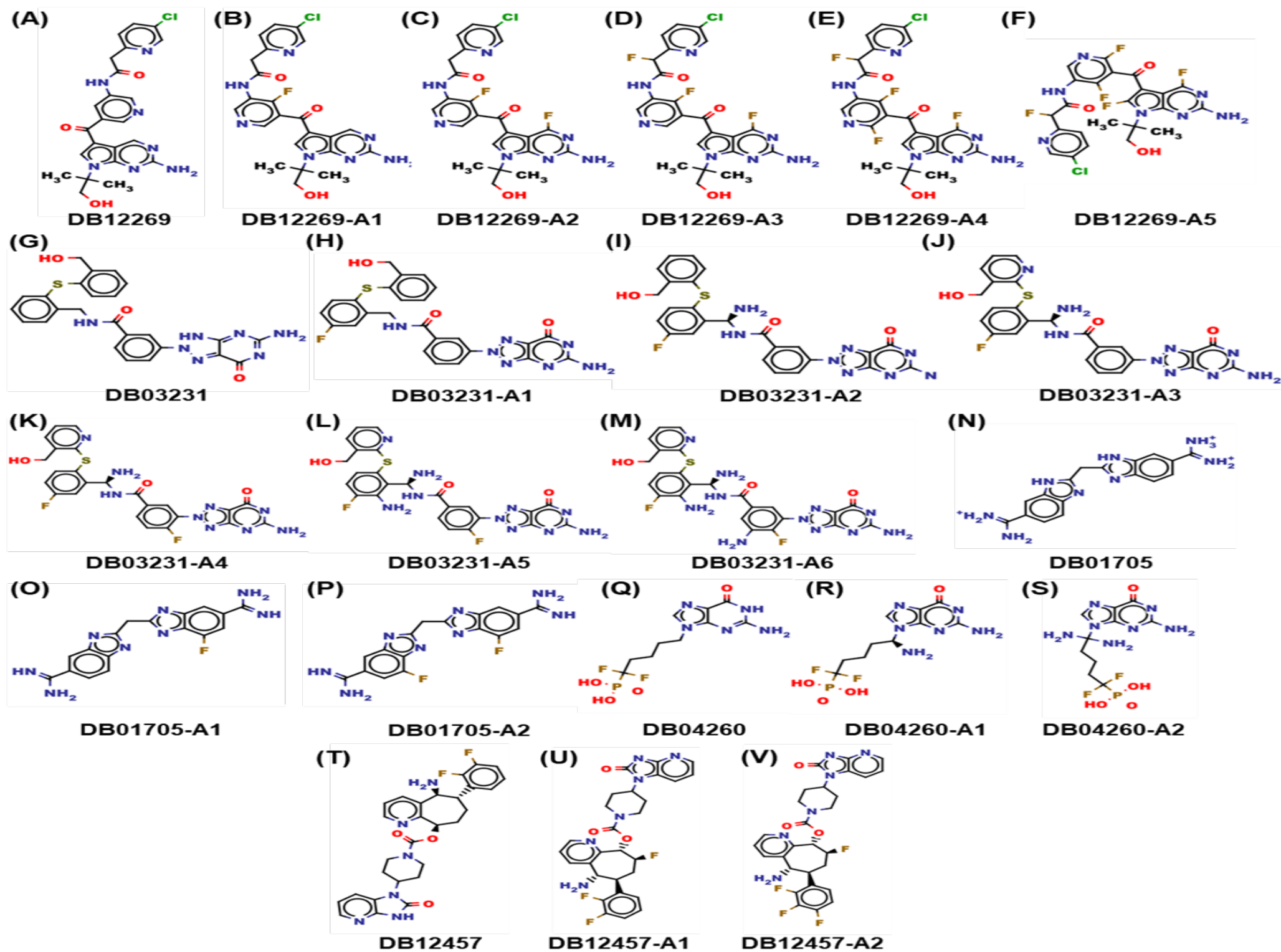


Fig: 12

Flowchart to Lead Analog compound generation

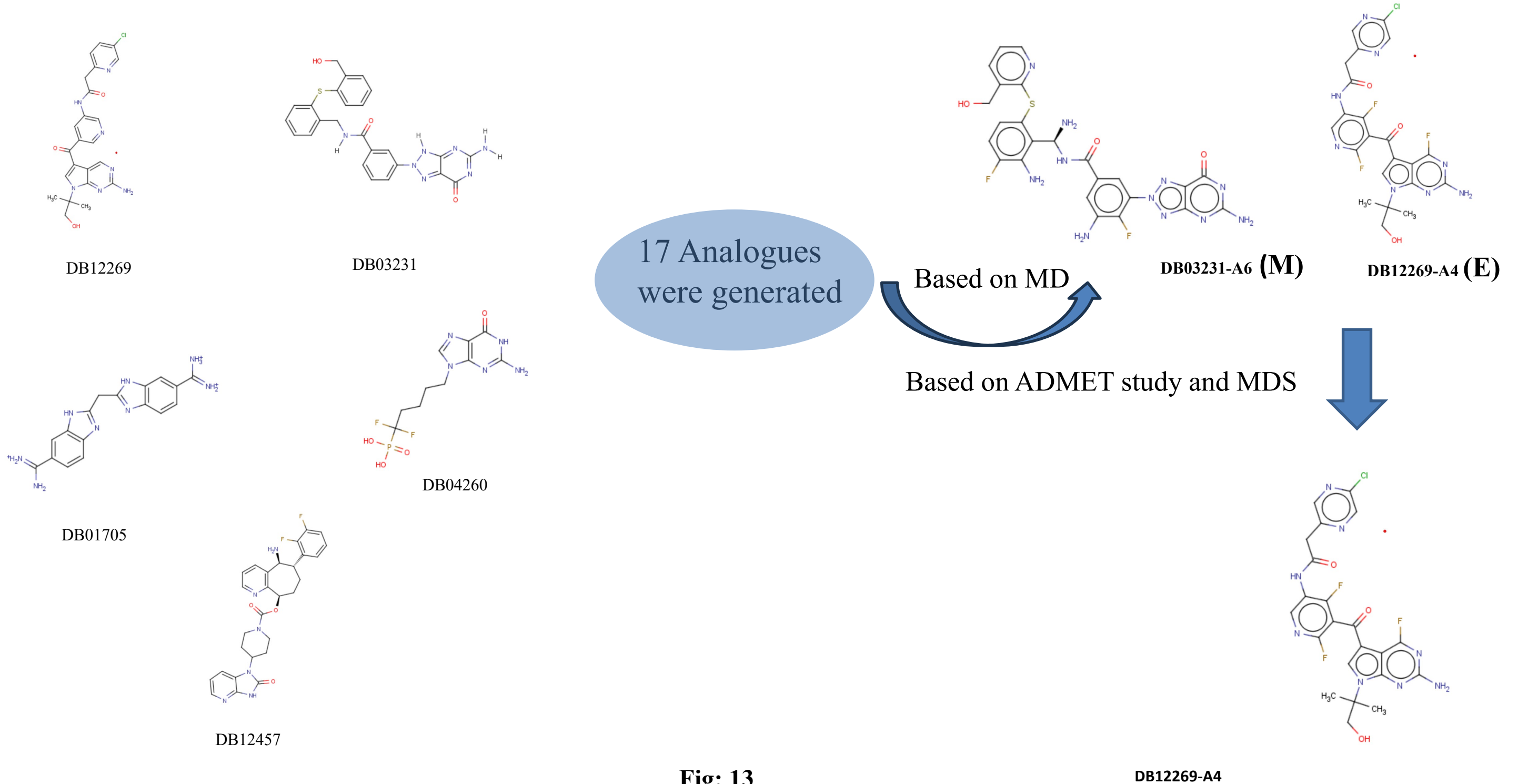


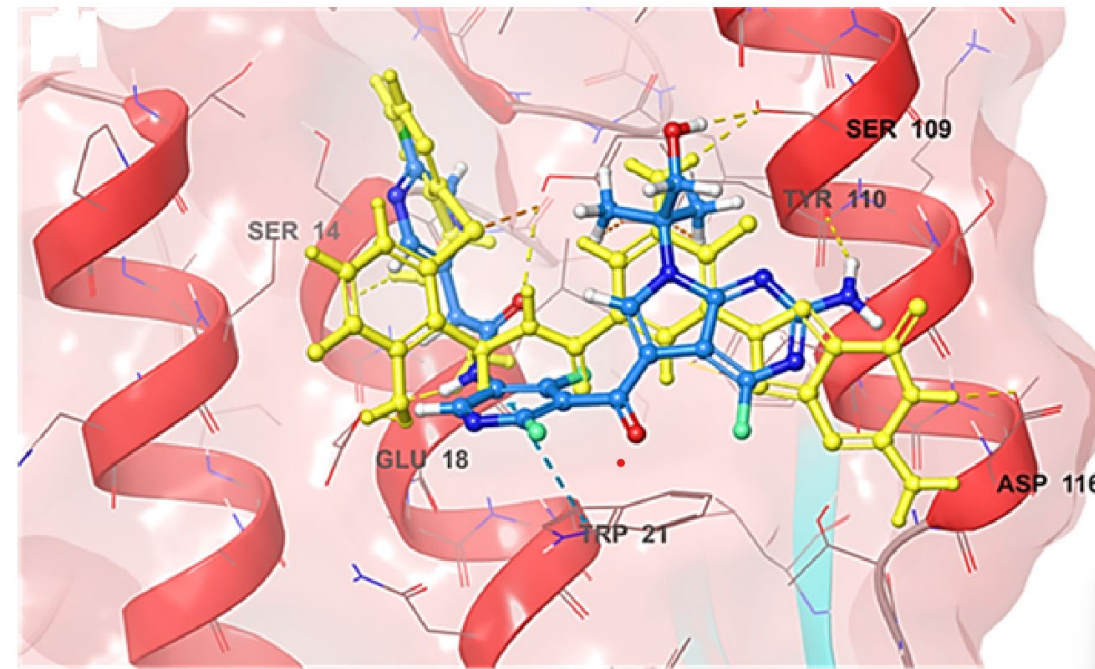
Fig: 13

DB12269-A4

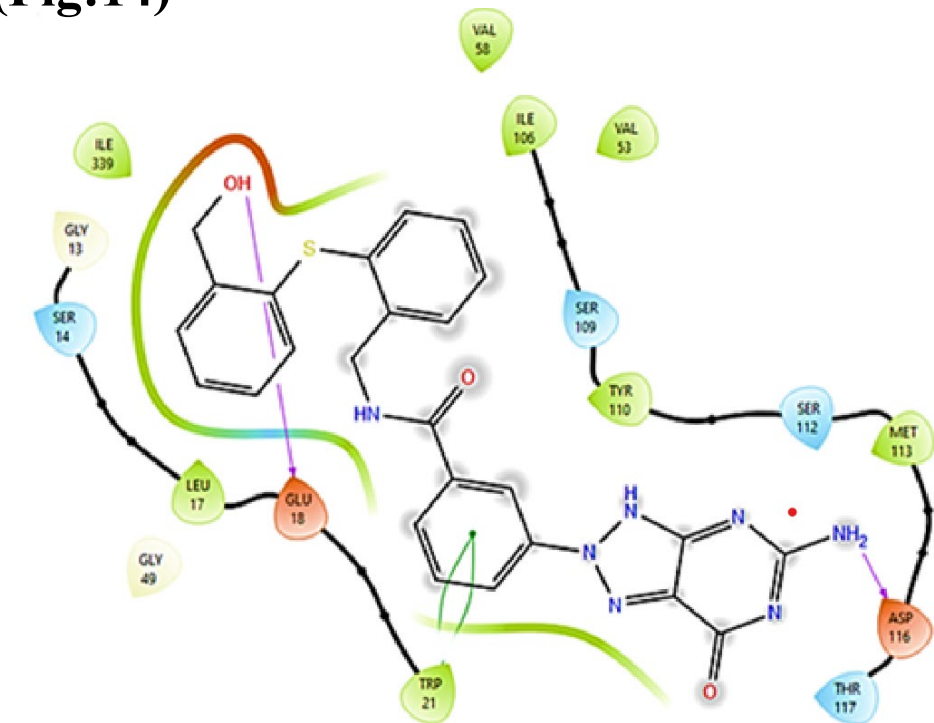
Depiction of Binding score of parent lead and their derivatives along with the binding pose and 2D interaction (Fig:14)

Table: 4

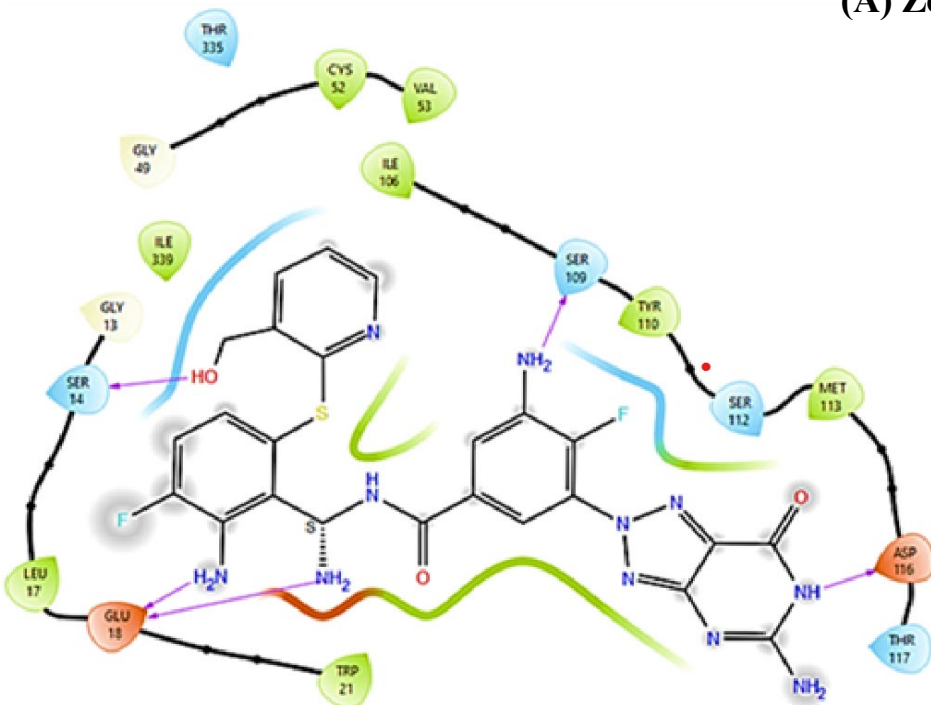
DrugBank ID	G(kcal/mol)
DB03231	-6.06
DB03231-A6	-6.80
DB12269	-6.58
DB12269-A4	-6.67
TRL190	-4.70



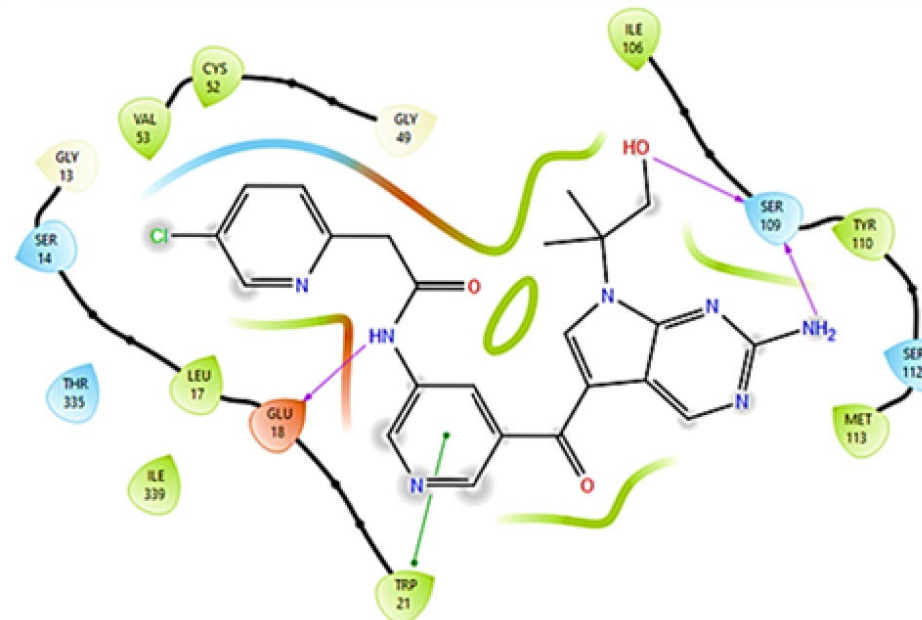
(A) Zoomed view depicting the best docked pose of DB03231-A6 and DB12269-A4 at the TR binding site



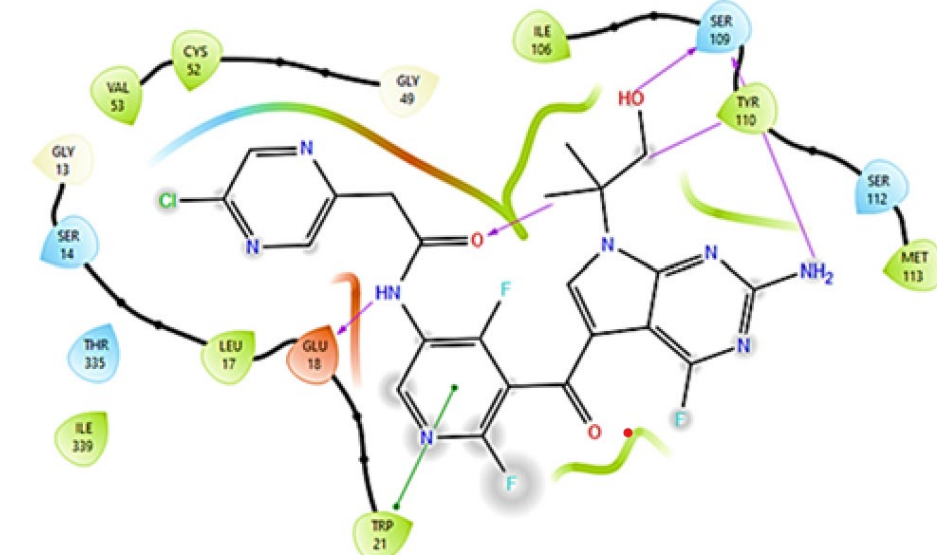
(B) 2D protein-ligand interactions as traced in DB03231



(B1) 2D protein-ligand interactions as traced in DB03231-A6



(C) 2D protein-ligand interactions as traced in DB12269



(C1) 2D protein-ligand interactions as traced in DB12269-A4

ADMET STUDY

Table: 5

Property / Parameter / Endpoint	DB12269-A4	DB03231-A6
Water solubility (log mol/L)	-2.989	-2.907
Caco2 permeability (log Papp in 10 ⁻⁶ cm/s)	0.936	0.962
Intestinal absorption (% Absorbed)(human)	75.855	46.7
Skin Permeability (log Kp)	-2.735	-2.735
Hepatotoxicity	0.52	0.52
Carcinogenicity	0.59	0.63
Mutagenicity	0.64	0.55
Cytotoxicity	0.72	0.72
Predicted LD50 (mg/kg)	2500	2000
Toxicity Class	5	4

Analysis of C α RMSD

The top-docked poses of DB03231-A6 and DB12269-A4 in complex with Trypanothione reductase underwent MDS and were analysed to find the best Analog compound through RMSD and RMSF analysis

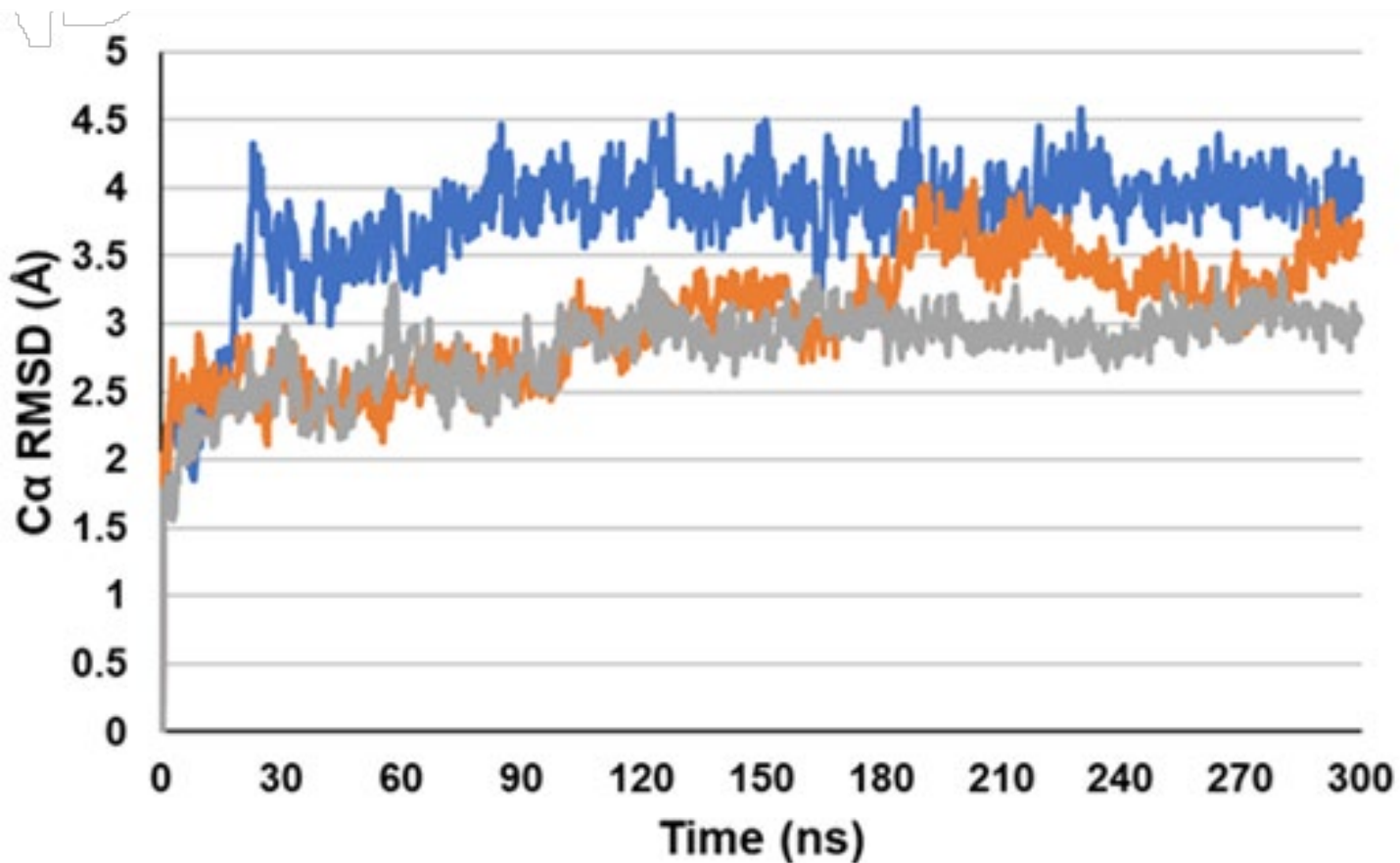


Fig: 15 (A) Protein C α RMSD

- The RMSD_{mean} of the C α atoms in the DB03231-A6-TR and DB12269-A4-TR complexes were significantly lower (3.04Å and 2.81Å, respectively) compared to the apo-TR form (3.77 Å).
- RMSD trajectories were consistent up to 177ns, after which DB03231-A6-TR exhibited more fluctuations than DB12269-A4-TR.
- Beyond 100ns, the apo-TR showed reduced fluctuations with a maximum RMSD difference of 1.40Å.
- DB12269-A4-TR demonstrated even lower fluctuations (0.78Å), while DB03231-A6-TR exhibited fluctuations (1.45Å) comparable to those observed in the apo-TR form.

Analysis of Protein Ligand RMSD

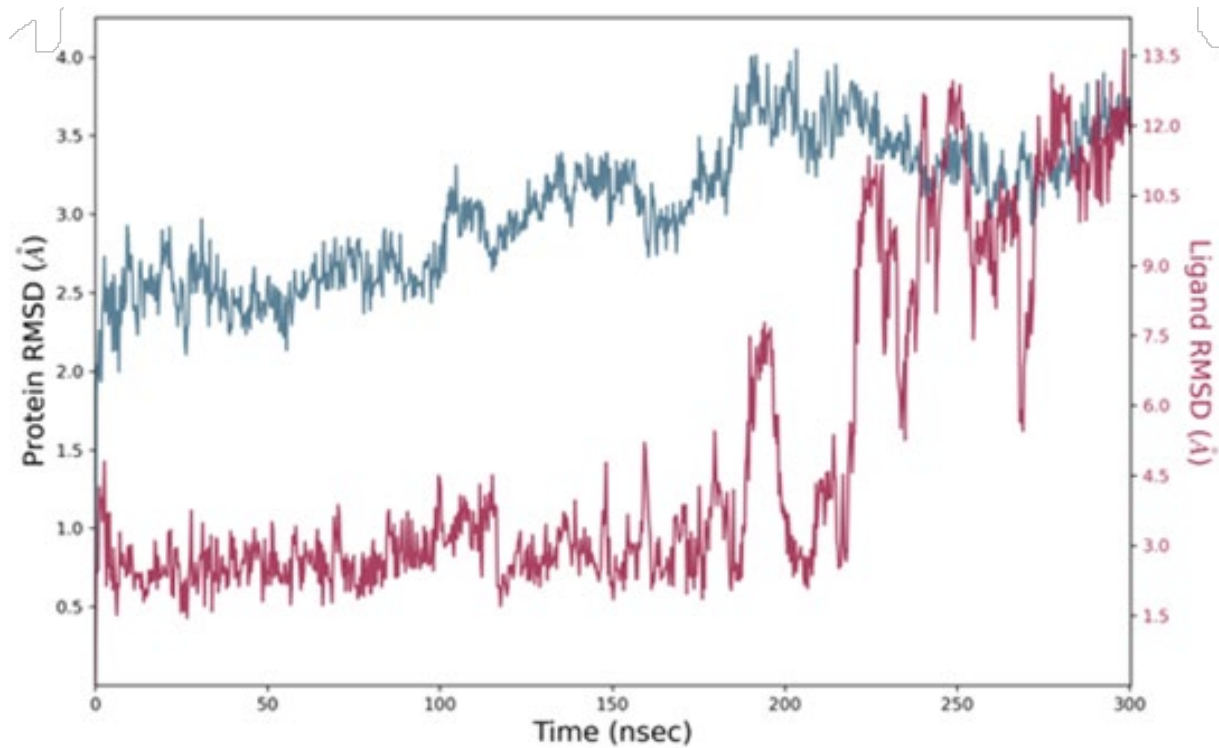


Fig: 15(B) Protein-ligand RMSD of DB03231-A6

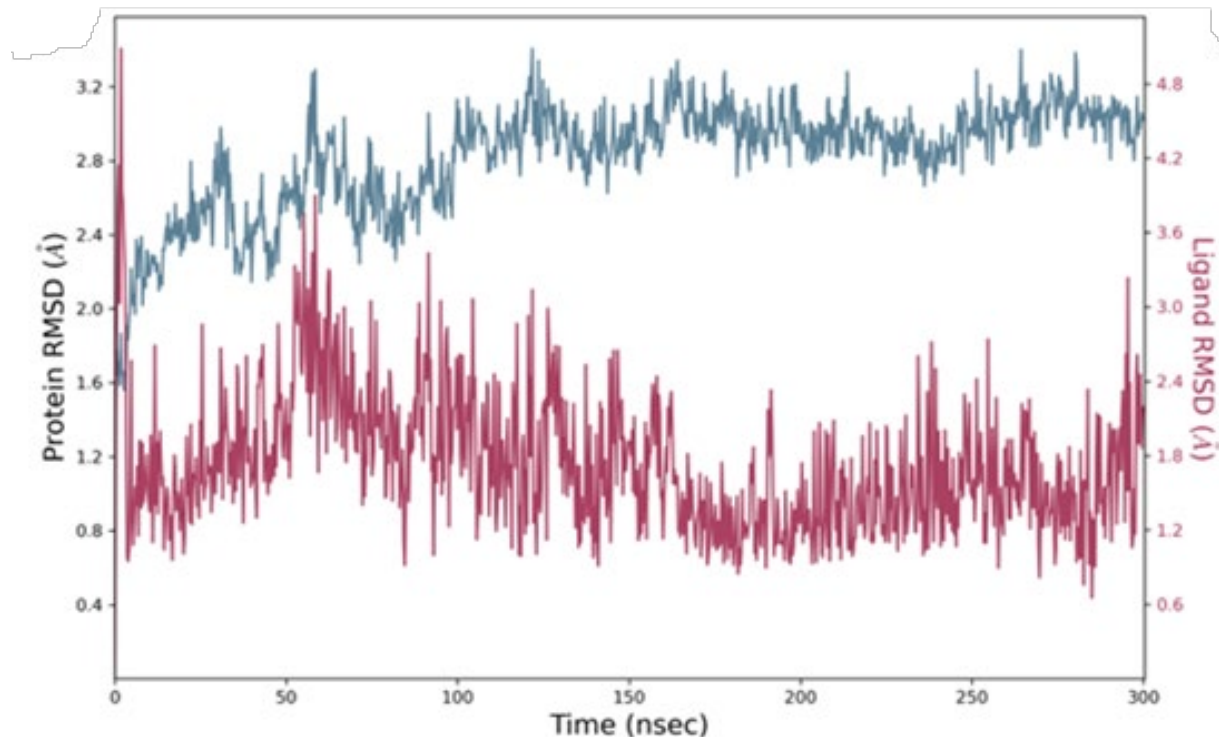
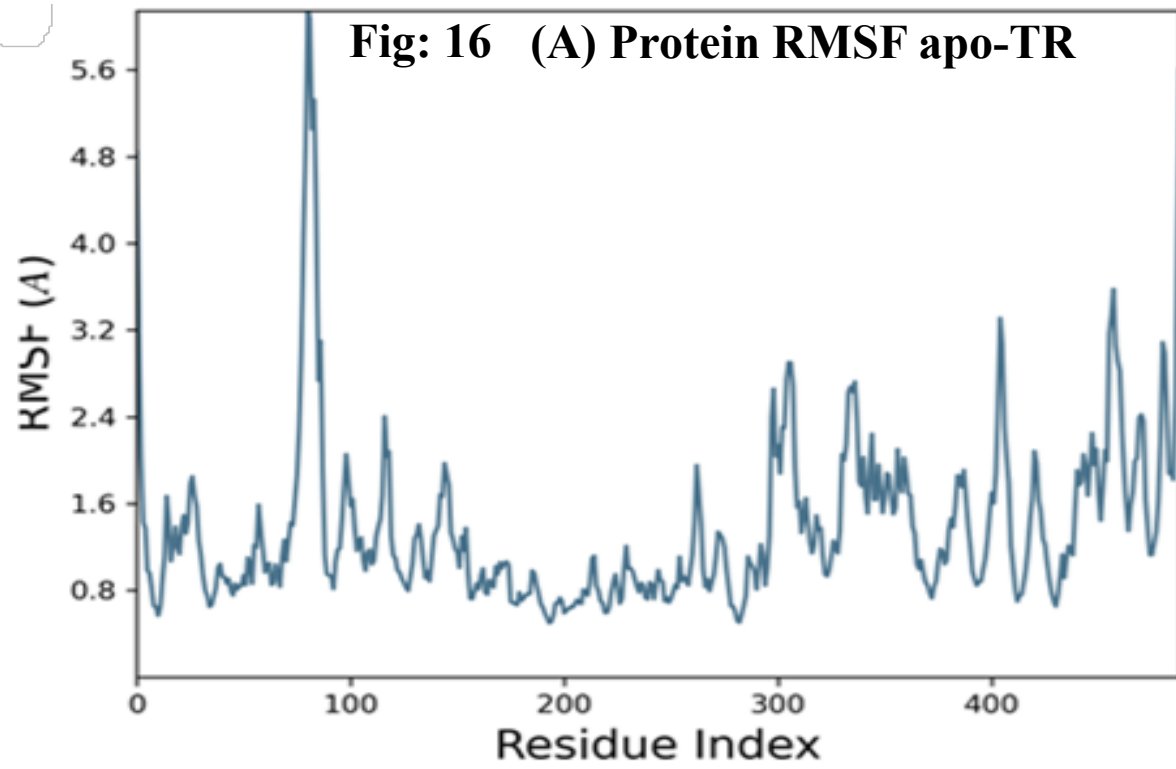


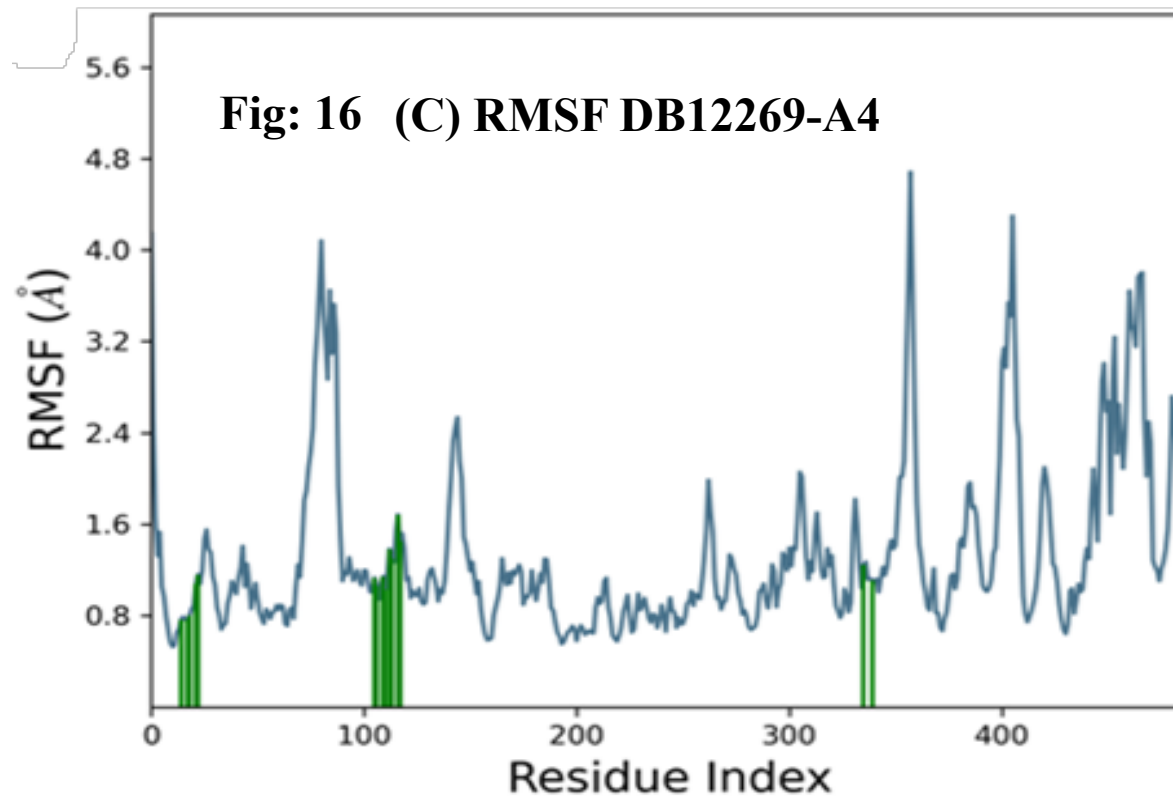
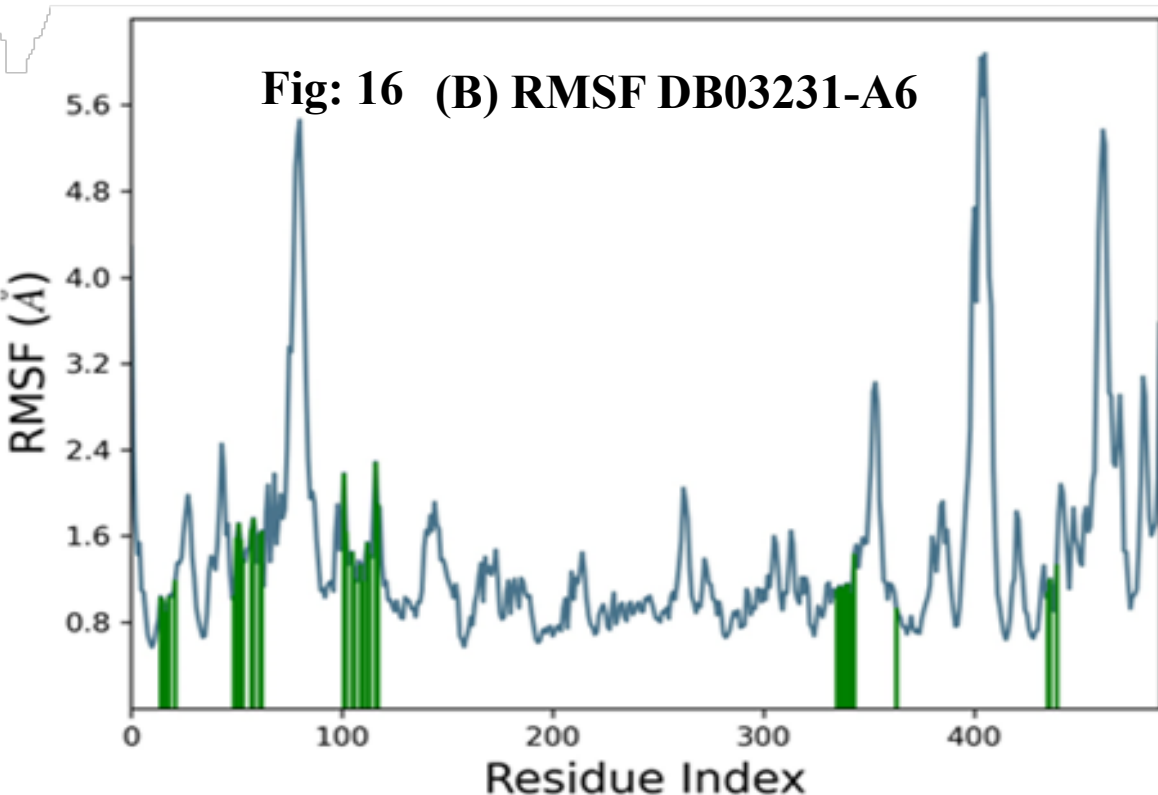
Fig: 15(C) Protein-ligand RMSD of DB12269-A4

- Superior stability of DB12269-A4 at the binding site was observed throughout the simulations.
- The average RMSD difference relative to TR was notably higher for DB03231-A6 (2.91Å) compared to DB12269-A4 (1.15Å),
- After 179 ns, DB03231-A6 exhibited significant fluctuations, although the protein-ligand trajectory converged towards the end of the simulation.
- Conversely, the ligand trajectory of DB12269-A4 did not overlap with the TR trajectory; however, the ligand distance from the binding site remained within the acceptable range (<3.5Å).

Analysis of protein ligand RMSF



- It is found that there are fewer interacting amino acid residues, exist with DB12269-A4.
- Still significant reduction in the flexibility of the target site amino acids is observed more effectively than DB03231-A6.



Analysis of protein-ligand contacts For DB12269-A4

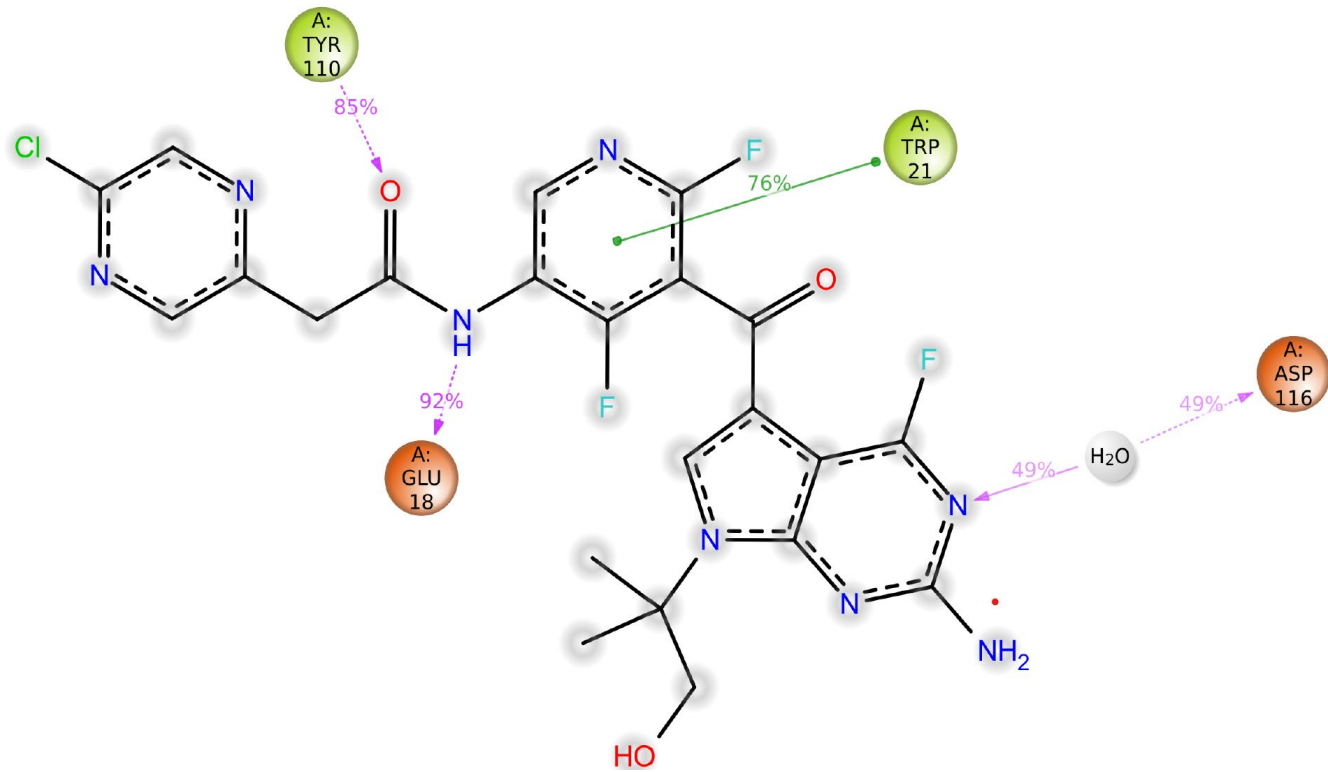


Fig: 17 (A) Ligand atom interactions with the protein residues

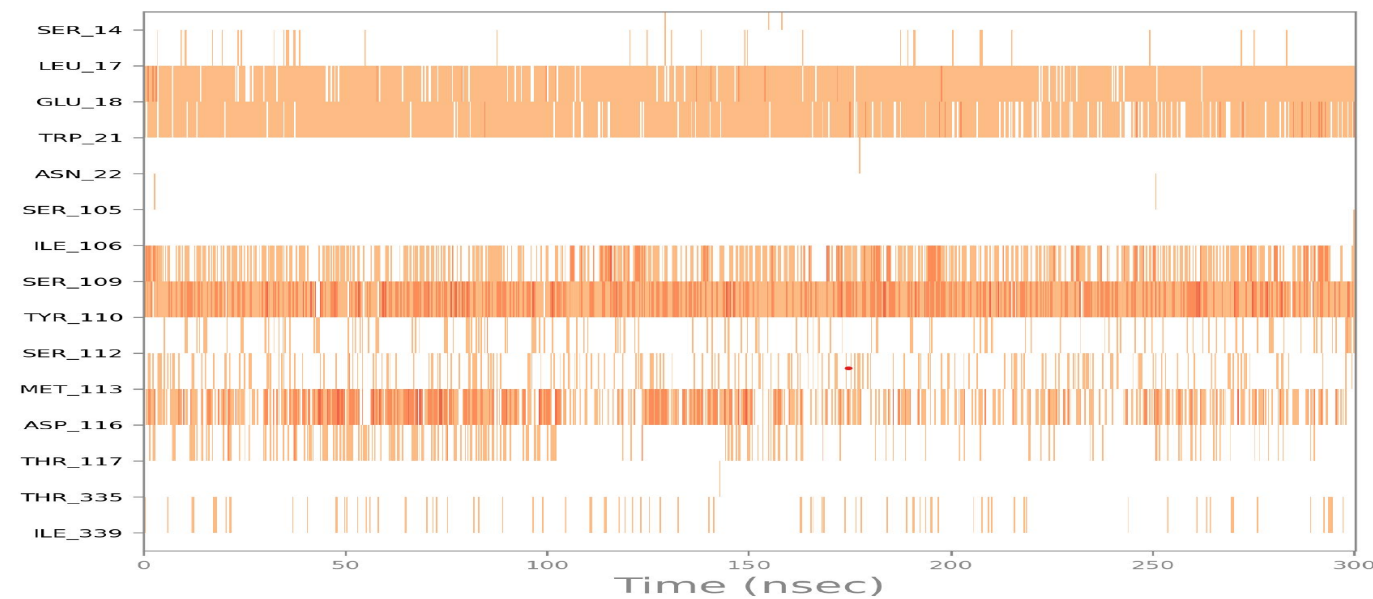


Fig: 17 (B) Interactions and contacts

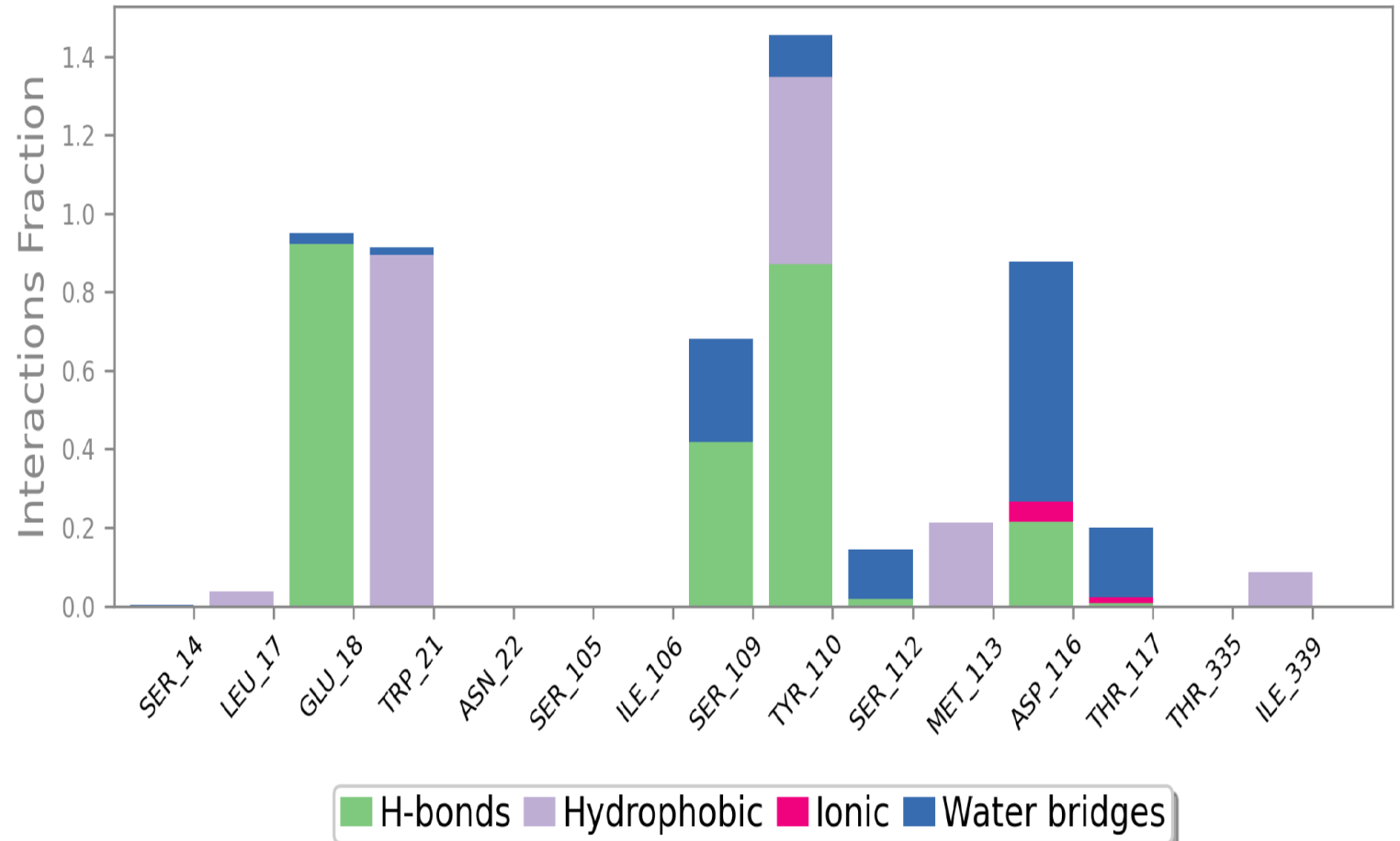


Fig: 17 (C) Type of interactions with ligand

- DB12269-A4 complex exhibited stable interactions with Tyr110 (85%), Trp21 (76%), and Glu18 (92%).
- And water-mediated hydrogen bonding with Asp116 (49%), indicating superior stability.

Analysis of protein-ligand contacts For DB03231-A6

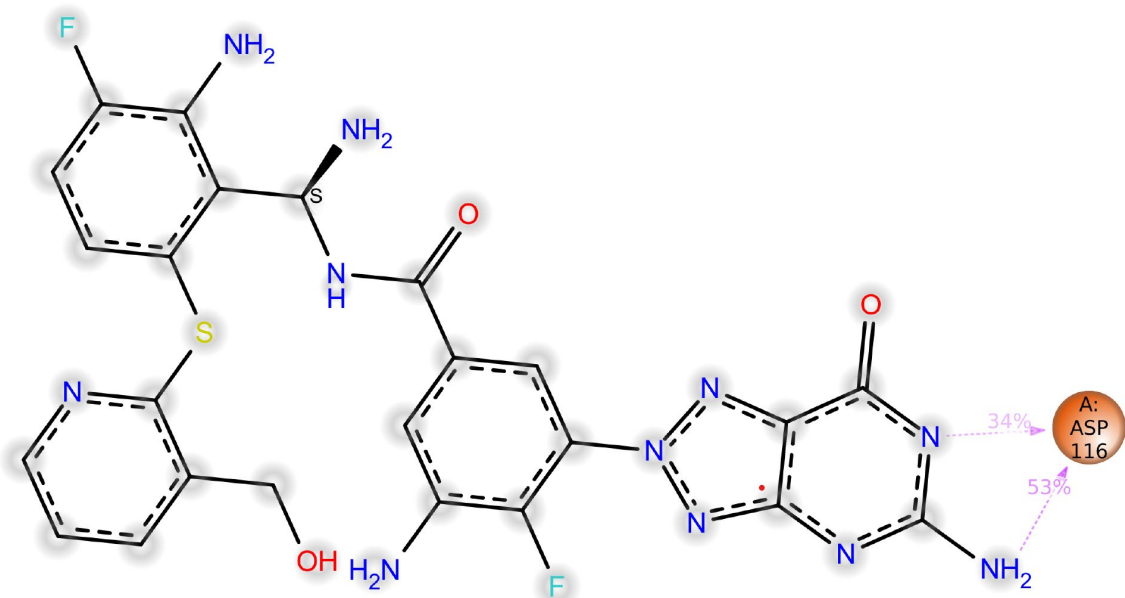


Fig: 18 (A) Ligand atom interactions with the protein residues

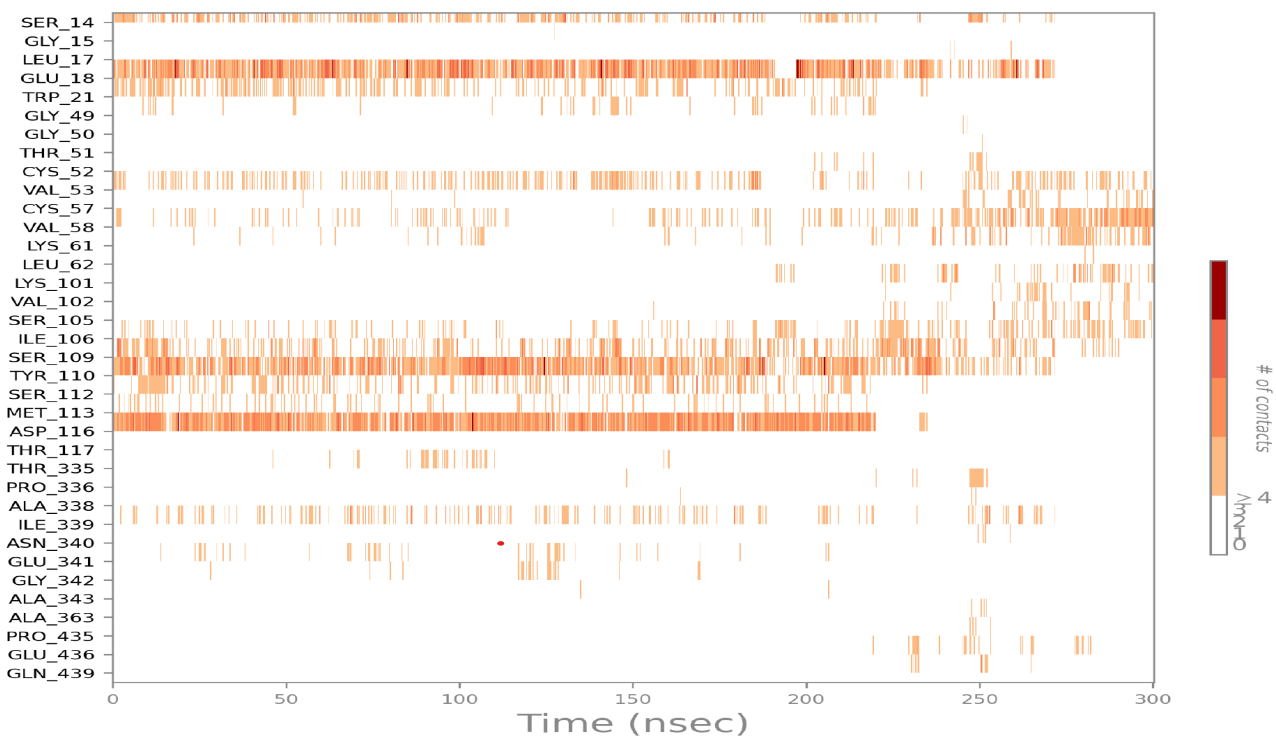


Fig: 18 (B) Interactions and contacts

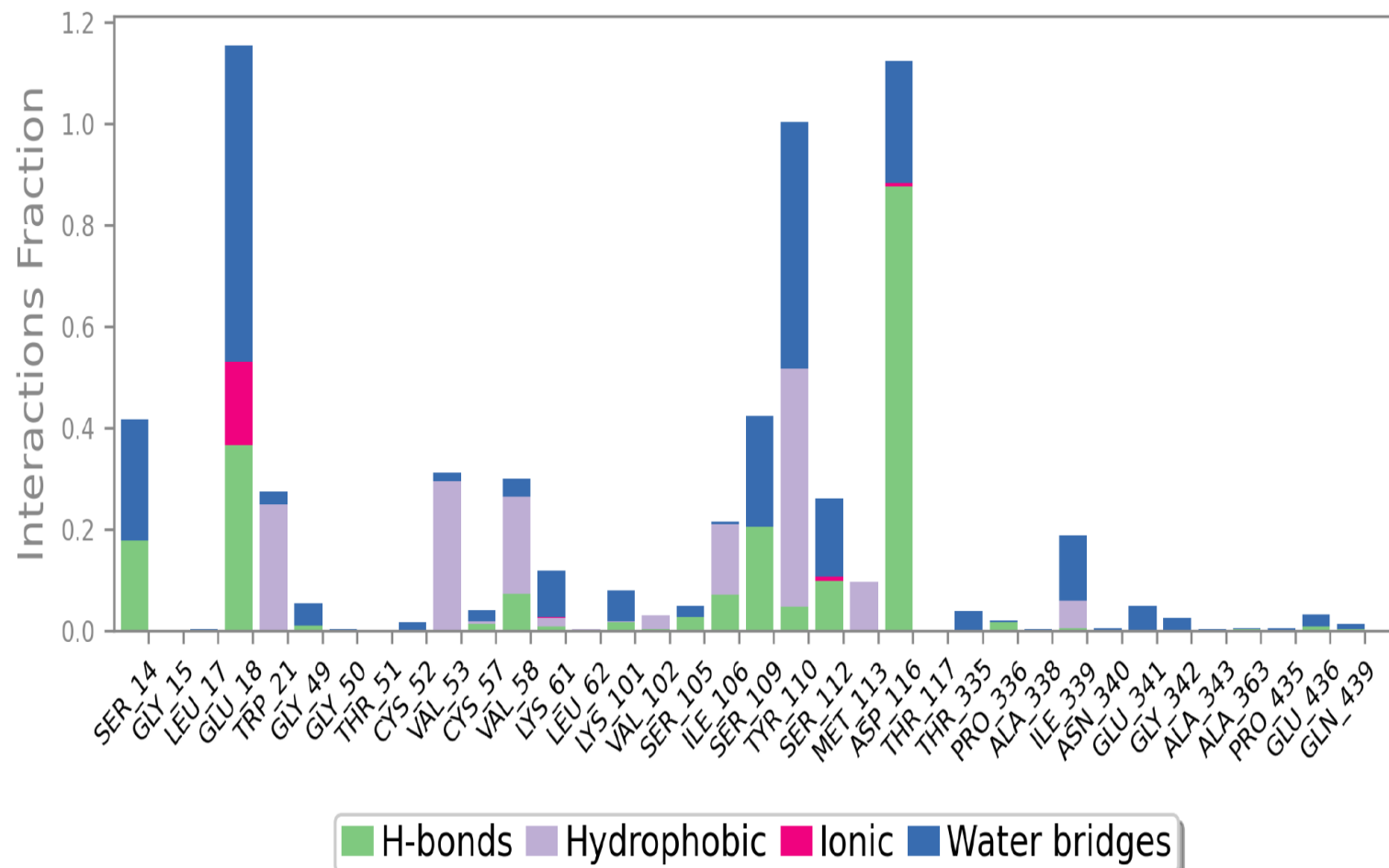


Fig: 18 (C) Type of interactions with ligand

- DB03231-A6 complex, the **nitrogen** atom and the attached **amine group** of the 5-amino-[1,2,3]triazolo[4,5-d]pyrimidin-7-one moiety.
- Formed hydrogen bonds with Asp116 for 34% and 53% of the simulation time, respectively.

Conclusion

- From QSAR model development the structural features revealed that descriptors like F03[C-N], F06[N-F], and Eta_F_A contributes positively in designing the structure and presence of B10[C-N] significantly reduces the efficacy of the compound designed.
- The developed model was deployed to reliably screen 12557 DrugBank compounds which enabled identification of the top five lead compounds i.e. DB12269, DB03231, DB01705, DB04260 and DB12457.
- The current study effectively utilizes simple, interpretable 2D molecular descriptors in QSAR modeling to predict TR inhibitory activity of 2-aminobenzimidazole derivatives with prospective lead modification.
- Positive descriptor features were incorporated and negative features were reduced to further potentiate the screened leads, resulting in the generation of 17 lead analogs.
- Finally through multi-layered screening involving inverse molecular docking and molecular dynamics revealed DB12269-A4 as the most promising TR inhibitor for leishmaniasis.

References

- Ghosh, V., Bhattacharjee, A., Kumar, A. and Ojha, P.K., 2024. q-RASTR modelling for prediction of diverse toxic chemicals towards *T. pyriformis*. SAR and QSAR in Environmental Research, 35(1), pp.11-30.
- Roy, K., Kar, S. and Das, R.N., 2015. Understanding the basics of QSAR for applications in pharmaceutical sciences and risk assessment. Academic press.
- Lipinski, C.A., 2004. Lead-and drug-like compounds: the rule-of-five revolution. Drug discovery today: Technologies, 1(4), pp.337-341.
- Finally through multi-layered screening involving inverse molecular docking and molecular dynamics revealed DB12269-A4 as the most promising TR inhibitor for leishmaniasis.
- Podder, T., Kumar, A., Bhattacharjee, A. and Ojha, P.K., 2023. Exploring regression-based QSTR and i-QSTR modeling for ecotoxicity prediction of diverse pesticides on multiple avian species. Environmental Science: Advances, 2(10), pp.1399-1422.

THANK YOU...